

# 1 Northward shift of boreal tree cover 2 confirmed by satellite record

## 3 Authors

5 Min Feng<sup>1,2</sup>; Joseph O. Sexton<sup>1</sup>; Panshi Wang<sup>1</sup>; Paul M. Montesano<sup>3,4</sup>; Leonardo Calle<sup>5</sup>; Nuno Carvalhais<sup>6,7</sup>;  
6 Benjamin Poulter<sup>8,9</sup>; Matthew J. Macander<sup>10</sup>; Michael A. Wulder<sup>11</sup>; Margaret Wooten<sup>3,12</sup>; William Wagner<sup>3,12</sup>; Akiko  
7 Elders<sup>13</sup>; Saurabh Channan<sup>1</sup>; Christopher S.R. Neigh<sup>3,12</sup>

## 8 Affiliations

10 <sup>1</sup> terraPulse, Inc., North Potomac, Maryland, USA.

11 <sup>2</sup> Institute of Tibetan Plateau Research, Chinese Academy of Sciences; Beijing, China.

12 <sup>3</sup> NASA Goddard Spaceflight Center; Greenbelt, Maryland, USA.

13 <sup>4</sup> ADNET Systems, Inc.; Bethesda, Maryland, USA.

14 <sup>5</sup> calleEcology, Inc., Missoula, MT, USA.

15 <sup>6</sup> Max Planck Institute for Biogeochemistry, Jena, Germany.

16 <sup>7</sup> Departamento de Ciências e Engenharia do Ambiente, DCEA, Faculdade de Ciências e Tecnologia, FCT,  
17 Universidade Nova de Lisboa, Caparica, Portugal.

18 <sup>8</sup> Spark Climate Solutions, San Francisco, California, USA.

19 <sup>9</sup> Department of Geographical Sciences, University of Maryland, College Park, Maryland, USA.

20 <sup>10</sup> ABR, Inc.—Environmental Research & Services, Fairbanks, Alaska, USA.

21 <sup>11</sup> Canadian Forest Service (Pacific Forestry Centre), Natural Resources Canada, 506 West Burnside Road, Victoria,  
22 British Columbia, Canada.

23 <sup>12</sup> Science Systems Applications, Inc., Lanham, Maryland, USA.

24 <sup>13</sup> Morgan State University, Baltimore, Maryland, USA.

26 Correspondence to: Min Feng ([mfeng@terrapulse.com](mailto:mfeng@terrapulse.com)), Joseph O. Sexton ([sexton@terrapulse.com](mailto:sexton@terrapulse.com))

27

28 **Abstract.** The boreal forest has experienced the fastest warming of any forested biome in recent decades. While  
29 vegetation–climate models predict a northward migration of boreal tree cover, the long-term studies required to test  
30 the hypothesis have been confined to regional analyses, general indices of vegetation productivity, and data calibrated  
31 to other ecoregions. Here we report a comprehensive test of the magnitude, direction, and significance of changes in  
32 the distribution of the boreal forest based on the longest and highest-resolution time-series of calibrated satellite maps  
33 of tree cover to date. From 1985 to 2020, boreal tree cover expanded by 0.844 million km<sup>2</sup>, a 12% relative increase  
34 since 1985, and shifted northward by 0.29° mean and 0.43° median latitude. Gains were concentrated between 64°–  
35 68°N and exceeded losses at southern margins, despite stable disturbance rates across most latitudes. Forest age  
36 distributions reveal that young stands (up to 36 years) now comprise 15.4% of forest area and hold 1.1–5.9 Pg of  
37 aboveground biomass carbon, with the potential to sequester an additional 2.3–3.8 Pg C if allowed to mature. These  
38 findings confirm the northward advance of the boreal forest and implicate the future importance of the region’s  
39 greening to the global carbon budget.

40

## 41 1 Introduction

42 The boreal biome is Earth’s most expansive and ecologically intact forest. The region contains  $38 \pm 3.1$  Pg Carbon  
43 (C) of above-ground biomass (Neigh et al., 2013) and is underlain by 1672 Pg C, summing to total biomass rivaling  
44 the tropics and half of global soil C (Gauthier et al., 2015). Its forested area comprises a third of the global total and  
45 accounts for 20.8% of the total forest carbon (C) sink (Pan et al., 2011; Pan et al., 2024). Boreal tree cover also controls  
46 the reflective and thermal balance of solar radiation of the high northern latitudes, posing a positive feedback  
47 mechanism for greenhouse atmospheric warming (Betts, 2000; Bonan, 2008; Chen et al., 2018; Randerson et al.,  
48 2006).

49 The boreal region has experienced the fastest climatological warming of any forest biome, with annual  
50 surface temperatures increasing more than 1.4° C over the past century (IPCC, 2014; IPCC, 2023). Boreal forest  
51 dynamics are highly correlated to climate (Elmendorf et al., 2012; Holtmeier and Broll, 2005; Véga and St-Onge,  
52 2009), and increases in vegetation productivity have been observed across the northern high latitudes (Berner and  
53 Goetz, 2022). However, regional increases in the frequency and severity of windthrow, fire, insect, and disease events  
54 have also been reported (Gauthier et al., 2015; Walker et al., 2019), and a recent analysis by Rotbart et al. (2023)  
55 suggests that southern contraction exceeds northern expansion, yielding net shrinkage of the boreal forest.

56 While theory predicts a northward shift of the boreal forest, the global net effects of climate and other factors  
57 on the density and distribution of its tree cover remain untested hypotheses at the spatial and temporal scale of Landsat,  
58 Earth’s longest-running record of global, high-resolution satellite imagery. Coupled climate-vegetation models predict  
59 a net-northward migration of boreal vegetation due to warming (IPCC, 2018; Scheffer et al., 2012), supporting the  
60 dominance of growth processes. Multiple studies (Berner and Goetz, 2022; Sulla-Menashe et al., 2018; Zhu et al.,  
61 2016; Piao et al., 2020) have reported vegetation “greening” (e.g., Berner and Goetz, 2022) based on spectral indices  
62 of plant productivity. However, the ecological effects of trees differ from those of graminoids, shrubs, and other  
63 vegetation, and the comparatively low productivity of boreal ecosystems necessitate long-term analyses that have

64 historically been limited to either regional scales or uncalibrated data (Beck et al., 2011; Brice et al., 2020; Taylor et  
65 al., 2017; Rotbart et al., 2023). As a result, the net effect of growth and mortality on the global distribution of boreal  
66 tree cover, and the resulting effect on carbon budgets, remain uncertain (Fan et al., 2023).

67 Here we report a global test of the magnitude and direction of boreal-forest change from 1985 to 2020, as  
68 observed through historical satellite records of tree cover calibrated to the boreal biome. We calibrated and expanded  
69 a global tree cover dataset (Carroll et al. 2011, Sexton et al., 2013) to 224,026 Landsat images estimating tree cover  
70 and its changes over the global extent of the boreal forest and adjacent tundra at annual, 30-meter resolution over 36  
71 years (Fig. S1)—the most extensive and highest-resolution record of boreal tree cover to date. This pan-boreal time  
72 series was then subjected to trend analysis to estimate and map the historical direction, rate, and significance of change  
73 across the region, and the resulting estimates of forest age were used to infer impacts on the region’s carbon budget.  
74

## 75 **2 Methods**

### 76 **2.1 Historical retrieval of tree cover**

77 To improve characterization of boreal forest structure, we calibrated the 250-m resolution, 2000 - 2020 MODIS  
78 Vegetation Continuous Fields (VCF) Tree Cover product (MOD44B Collection 6; Carroll et al., 2011) against a  
79 region-wide sample of airborne lidar measurements, stratifying by topographic and bioclimatic covariates  
80 (Supplemental Information (SI) §2–4). This boreal-specific calibration improved characterization of tree-cover  
81 gradients across the boreal region (Fig. S7), increasing accuracy, decreasing uncertainty, and improving the linear  
82 correlation of per-pixel fractional tree cover estimates to reference measurements (Fig. S8). Mean absolute error  
83 (MAE) decreased to 11.13%, root-mean-squared error (RMSE) decreased to 16.44%, and the coefficient of  
84 determination ( $R^2$ ) of the linear model between estimated and measured data increased to 0.60.

85 The calibrated MODIS VCF estimates were then downscaled to 30-m resolution and extended to 1984–2020  
86 by applying a machine learning model (gradient-boosted regression tree) to Landsat surface reflectance imagery from  
87 sensors Thematic Mapper (TM), Enhanced Thematic Mapper Plus (ETM+), and Operational Land Imager (OLI)  
88 (Sexton et al., 2013; SI §5–6). A total of 224,026 Landsat scenes across 2,189 World Reference System 2 (WRS-2)  
89 tiles was used to reconstruct annual tree cover estimates, composited to minimize cloud, snow, and phenological noise.  
90 For each pixel-year, the median value of valid observations was retained, resulting in a consistent, high-resolution  
91 time series of tree cover estimates (Fig. S5–S7). The residual bias of the Landsat-based estimates relative to the LiDAR  
92 reference measurements was slight (~2%, SI).

93

### 94 **2.2. Tree cover trend analysis**

95 The calibrated, downscaled, and extended tree cover values were then summarized across the region as annual, boreal-  
96 wide means and medians to calculate changes over the 36-year study span (Fig. 2). The annual mean and median tree  
97 cover were also broken down by latitude to calculate the change rate at each latitudinal degree between 47°N to 70°N  
98 (Fig. S10). Tree cover estimates for 1984 were excluded from the trend analysis due to the poor spatial coverage in  
99 the first operational year of Landsat 5 (Fig. S2), and pixels with less than 30 unobscured annual tree cover observations

100 were excluded to minimize unbalanced representation caused by the lapses in the availability of Landsat images,  
101 mainly in central and northeast Siberia (Neigh et al., 2013; Sexton et al., 2013).

102

### 103 **2.3. Detection of forest change and estimation of age**

104 Following the United Nations Framework Convention on Climate Change (UNFCCC, 2002), forest was defined as  
105 tree cover exceeding 30% within each 30-m pixel. The probability of a pixel being forested,  $p(F)$ , was calculated as  
106 the integral of the probability density function of tree cover values exceeding this 30% threshold (SI §11). Using the  
107 36-year time series of annual, 30-m resolution estimates of forest probability ( $p(F)$ ), forest changes, i.e., gains and  
108 losses, were identified by applying a two-sample z-test in a moving kernel centered on transitions across the 50%  
109 threshold of  $p(F)$  (Fig. S13).

110 Pixels with multiple statistically significant transitions during the 1985–2020 period were permitted up to  
111 three gain or loss events. Forest changes were classified as “incomplete” if more than 7 years of data were missing,  
112 and “complete” otherwise. Incomplete changes were concentrated in areas with sparse Landsat acquisitions prior to  
113 1999, before implementation of systematic global imaging by Landsat 7 (Sexton et al., 2013; Potapov et al., 2012).

114 Forest age was estimated for each year and pixel by subtracting the year of the most recent significant forest  
115 gain from the year of interest. Pixels were classified as “new” forests if no forest cover or loss had been observed  
116 earlier in the time series within a 150-m radius (five Landsat pixels); otherwise, forests were considered “recovering.”  
117 This approach does not capture the initial years of seedling establishment and growth when cover is below this  
118 detection threshold. Also, because of the limited Landsat period, areas detected as “new” forest may actually be  
119 “recovering” from pre-1985 disturbances. Accuracy of change detection and age estimation was assessed against a  
120 reference sample of 2,404 visually interpreted points distributed across the boreal biome (Fig. S14 and S15).

121

### 122 **2.4. Estimation of aboveground biomass**

123 Aboveground biomass carbon (AGB) was estimated as a function of forest stand age using a linear growth model  
124 (Cook-Patton et al., 2020; Fig. S16), with intercept ( $\mu = -35.7$ ,  $\sigma = 12.6$ ) and slope coefficients ( $\mu = 23.2$ ,  $\sigma = 3.2$ )  
125 incorporating parametric uncertainty. Because ages of forests older than the 36-year time-series could not be directly  
126 observed, we assumed three scenarios of stand age to bracket carbon stock estimates in these undated stands: the  
127 absolute minimum possible age (36 years) yielding 19.1–58.4 Pg C, and typical ages for mature and old-growth stands  
128 in boreal ecosystems, i.e., 100 years yielding 35.8–80.5 Pg C, and 300 years yielding 42.4–89.2 Pg C.

129 These scenarios define the plausible envelope of legacy biomass in mature forest. However, estimates  
130 reflected structural biomass only and did not account for potential effects of changes in soil moisture or variation in  
131 respiration rates. To contextualize the biomass sink relative to climate-driven emissions, we also evaluated the trend  
132 in regional surface air temperature using the Climate Research Unit (CRU) dataset and the European Centre for  
133 Medium-Range Weather Forecasts (ECMWF) ERA-Interim reanalysis. Both records indicated significant warming  
134 over the study period, with trends of  $0.038^{\circ}\text{C yr}^{-1}$  ( $r = 0.69$ ,  $p < 1 \times 10^{-5}$ ) and  $0.035^{\circ}\text{C yr}^{-1}$  ( $r = 0.73$ ,  $p < 1 \times 10^{-6}$ )  
135 respectively (Fig. S17).

136 **3 Results**

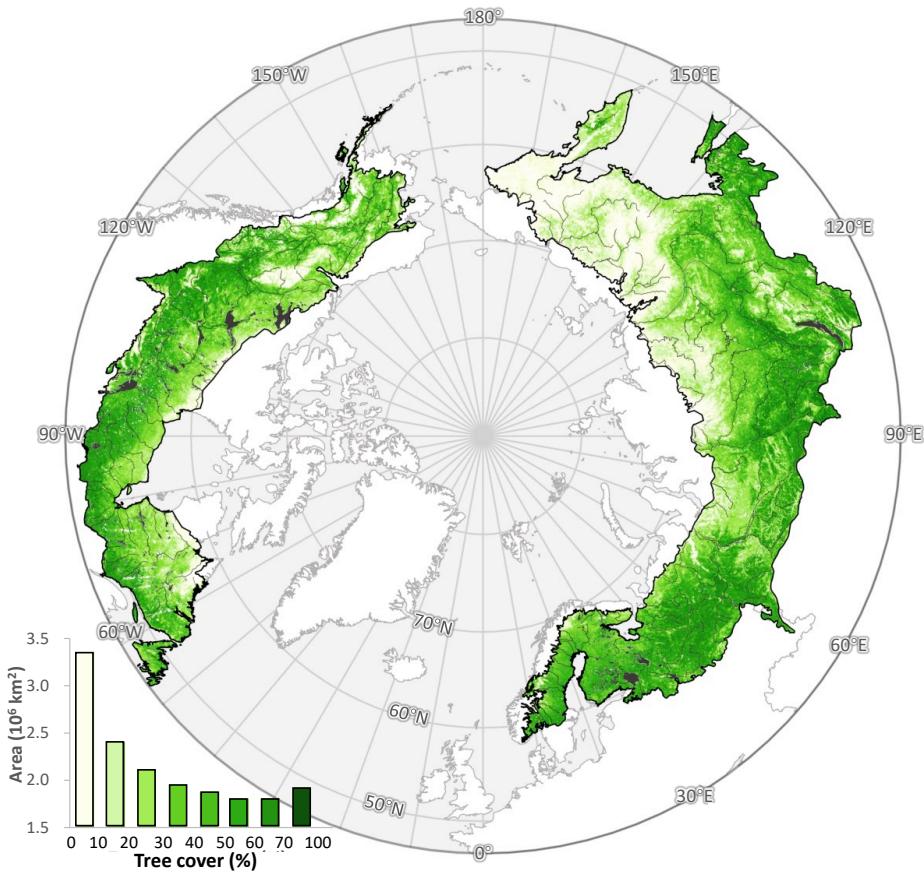
137 **3.1. Distribution of boreal tree cover**

138 Tree cover reaches its highest densities in the southern portion of the boreal biome and decreases progressively  
139 northward (Fig. 1). Sparse conifer stands, woodlands, herbaceous vegetation, and unvegetated barrens dominate the  
140 transition to Arctic tundra, and tree cover is nearly absent north of 71°N. Due to interspersion of tundra, wetlands, and  
141 inland water bodies, the most common local (i.e., 30-meter pixel) tree-cover density across the entire boreal forest and  
142 taiga-tundra ecotone is below 5%.

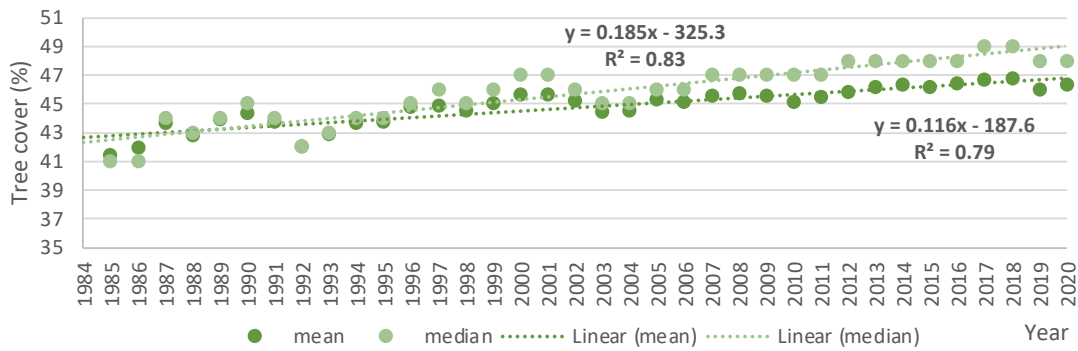
143 Boreal tree cover expanded from 7.153 million km<sup>2</sup> (41.44% of the region) in 1985 to 7.997 million km<sup>2</sup>  
144 (46.32%) in 2020, with a linear trend of 0.023 million km<sup>2</sup> yr<sup>-1</sup> (0.12% yr<sup>-1</sup>; percent cover = 0.116 × year – 187.6, R<sup>2</sup>  
145 = 0.99, p < 0.001) (Fig. 1). From 1985 to 2020, the boreal tree cover increased by 0.844 million km<sup>2</sup>, a 4.3 percentage  
146 point absolute increase and a 12% relative increase over its 1985 extent. Applying the UNFCCC forest definition of  
147 10–30% tree cover (UNFCCC, 2002; Sexton et al., 2016), the region held between 8.95 and 12.41 million km<sup>2</sup> of  
148 forest in 2000 and between 9.41 and 13.26 million km<sup>2</sup> in 2020.

149 The latitudinal distribution of tree cover also shifted northward from 1985 to 2020. The mean latitude of tree  
150 cover increased by 0.29°, from 57.37°N in 1985 to 57.66°N in 2020 (mean latitude = 0.0075 × year + 42.6, R<sup>2</sup> = 0.79,  
151 p < 0.001). The median latitude increased more rapidly, by 0.43° (median latitude = 0.0124 × year + 32.5, R<sup>2</sup> = 0.88,  
152 p < 0.001), indicating widespread net expansion across the biome rather than outliers of change at either its northern  
153 or southern extremes.

154



155



156

157 **Fig. 1. Distribution of boreal across boreal ecoregions in 2020. Estimates from 2020 are shown. Data gaps due to clouds**  
 158 **were filled with estimates from earlier years. Ecoregions were defined by Dinerstein et al (2017). The bottom panel shows**  
 159 **the increasing density in the overall, pan-boreal density of tree cover from 1985 to 2020.**

160

### 161 3.2. The pace and pattern of boreal forest change

162 Net biome-wide changes were underlain by strong geographic variation (Fig. 2). Net gains from 1985 to 2020 occurred  
 163 at all latitudes above 53°N, with the strongest increases concentrated between 64° and 68°N. Gains in the northernmost  
 164 latitudes support the hypothesis of a poleward shift in the northernmost extent of tree cover and are consistent with  
 165 findings by Montesano et al. (2024), who reported long-term increases in deciduous and mixed forest components in

166 transitional boreal zones. These structural shifts parallel recent evidence that warming-induced species diversification  
167 is strongest near the tundra margin as temperate species colonize newly viable habitat (Xi et al., 2024). In contrast,  
168 net losses were smaller in magnitude and limited to the southern boreal latitudes (47°–52°N), corroborating recent  
169 observations by Rotbart et al. (2023).

170 Our analysis of calibrated, high (30-meter) resolution estimates of tree cover minimized potential for  
171 herbaceous growth to obscure tree mortality, for which coarser-resolution, The Normalized Difference Vegetation  
172 Index (NDVI)-based analyses have been criticized (Yan et al., 2024). The pan-boreal expansion of tree cover occurred  
173 against relatively stable disturbance rates over the study period (Fig. 3), and observed disturbances influenced regional  
174 patterns but did not obscure the biome-wide trend. The annual rate of disturbance increased modestly from 53,546  
175  $\text{km}^2 \text{ yr}^{-1}$  in 2000 to 60,275  $\text{km}^2 \text{ yr}^{-1}$  in 2020, equivalent to a 1.8%  $\text{yr}^{-1}$  linear increase ( $1,100 \text{ km}^2 \text{ yr}^{-1}$ ), or approximately  
176 0.2%–0.4% of the forested area. Locations undisturbed between 1985 and 2020 exhibited net gains across nearly all  
177 latitudes, and the latitudinal distribution of disturbance—while varying strongly among years—remained broadly  
178 stationary over time. (Fig. S10).

179 In North America, the largest gains were concentrated in the northernmost boreal, where increases in shrubs  
180 and grasses have also been reported (McManus et al., 2012). Areas of net loss corresponded to widespread forest  
181 disturbances, including wildfire and bark beetle (*Dendroctonus* spp.) outbreaks in British Columbia (Meddens et al.,  
182 2012), spruce budworm (*Choristoneura* spp.) in Quebec (Boulanger and Arseneault, 2004), and wildfire across  
183 western Canada and interior Alaska (Stocks et al., 2002). Recent shifts in transitional forest structure and composition  
184 noted by Montesano et al. (2024) lend further weight to these observations, suggesting a biome-wide response in  
185 functional traits, including increased deciduous dominance at the taiga-tundra ecotone. These findings are also  
186 partially corroborated by Rotbart et al (2023), who also reported tree cover gains in the boreal interior of North  
187 America but loss at the southern margins, especially in areas impacted by wildfire and harvest.

188 In Eurasia, hotspots of forest loss included the eastern Russian–Chinese border, agricultural zones south of  
189 the Urals, and regions affected by timber harvesting near the Russia–Finland border in the 1990s (Potapov et al.,  
190 2012). Logging and fire contributed to localized loss in eastern Russia (Krylov et al., 2014), whereas gains in northern  
191 Europe were associated with silvicultural management, afforestation, and fire suppression (Henttonen et al., 2017).  
192 Recent analyses confirm extensive regrowth in post-agricultural and permafrost-transitioning landscapes in Russia,  
193 where lidar and optical remote sensing reveal increases in regeneration potential, particularly in abandoned or  
194 disturbed sites (Neigh et al., 2025).

195 In Asia, net gains were observed in areas of post-Soviet agricultural abandonment, as well as in larch forests  
196 near the Yakutsk permafrost zone. These trends are consistent with increases in tall shrubs and larch (*Larix* spp.) at  
197 the taiga–tundra boundary (Frost and Epstein, 2014). Recovery from wildfires in the 1990s continues in these regions  
198 (Kajii et al., 2002), and permafrost thaw has been hypothesized to enhance productivity (Sato et al., 2016).

199 Although we did not attempt to demarcate or detect changes in a discrete tree line, our observations  
200 corroborate the boreal advancement hypothesis alongside field measurements of woody vegetation near the northern  
201 limits of tree growth and satellite-based studies demarcating the northern tree line (Frost and Epstein, 2014; Rees et  
202 al., 2020; Dial et al., 2024; Dial et al., 2022; Rotbart et al. 2023). While analysis of tree-cover estimates avoided the

203 potential confusion of changes in trees specifically with general NDVI-based “greening” (Yan et al. 2024), the trend’s  
204 geographic variations correspond to general patterns of greening across the biome (Berner and Goetz, 2022; Sulla-  
205 Menashe et al., 2018; Zhu et al., 2016; Piao et al., 2020; Guay et al., 2014).

206 Field studies have shown that climate, soil properties, and forest management drive large differences in boreal  
207 tree growth rates across the ecotone (Henttonen et al., 2017; Henttonen et al., 2017; Hofgaard et al., 2009). Recent  
208 shifts in transitional forest structure and composition noted by Montesano et al. (2024) lend further weight to these  
209 observations, suggesting a total biome-wide response in functional traits, including increased deciduous dominance  
210 near treeline margins. Xi et al. (2024) further demonstrate that increasing diversity near the forest–tundra boundary is  
211 associated with moderate climatic warming, although they caution that the gains are vulnerable to reversal under  
212 extremes such as drought and heatwaves. Changes in species composition remain a focal point of research (Xi et al.,  
213 2024; Mekonnen et al., 2019; Massey et al., 2023; Mack et al., 2021; Liski et al., 2003), while still remaining to be  
214 explored are the differentiation of climate and soil effects at the global scale and the discrimination of tree cover  
215 expansion due to the establishment and growth of new seedlings versus the widening of existing tree crowns.

216

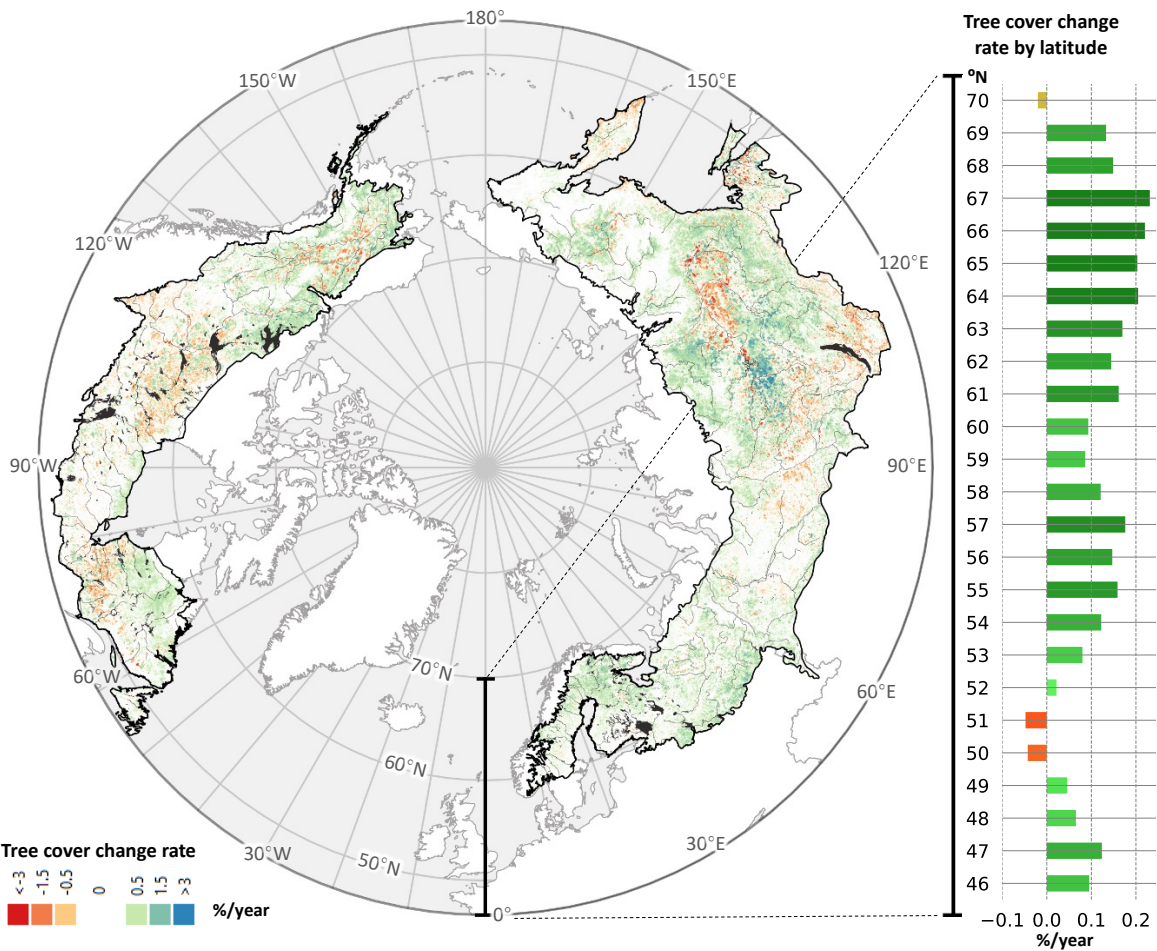
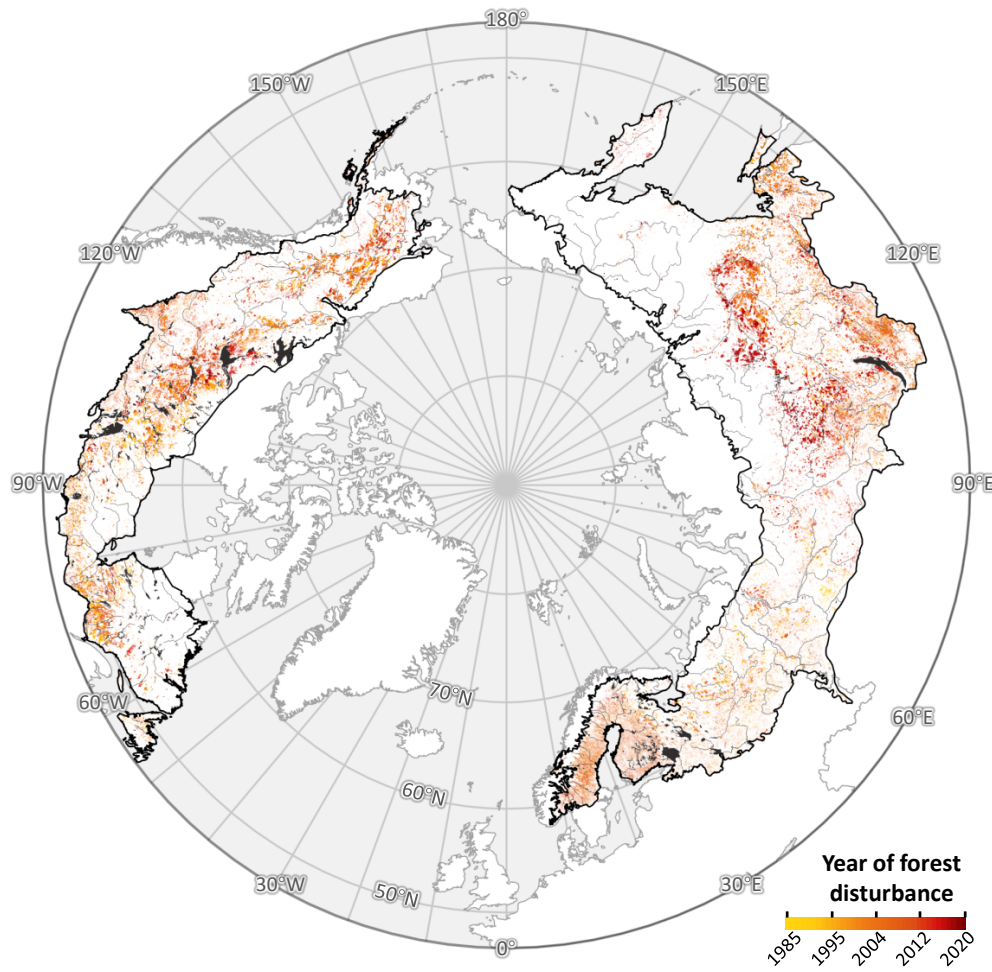


**Fig. 2. Spatial and temporal distribution of boreal tree cover change from 1985 to 2020.** Map: significant net gains (green-blue) and losses (orange-red) of tree cover over the boreal biome. Bar chart (top-right): linear regression slope of tree cover over time, stratified by latitude. Time series (bottom): northward migration of the distribution of mean and median latitude of tree cover. Every 30-m resolution pixel included in the analysis had >30 unobscured annual tree cover estimates between 1985 and 2020.



225



226

227 **Fig. 3. Total area and median latitude of boreal stand-clearing disturbances from 1985 to 2020.** Trends are plotted for the  
228 portion of the boreal area where the satellite image is complete from 1984 to 2019 (“complete”) and from all locations,  
229 including where the satellite record is incomplete (“incomplete”) (Supplemental Information).

230

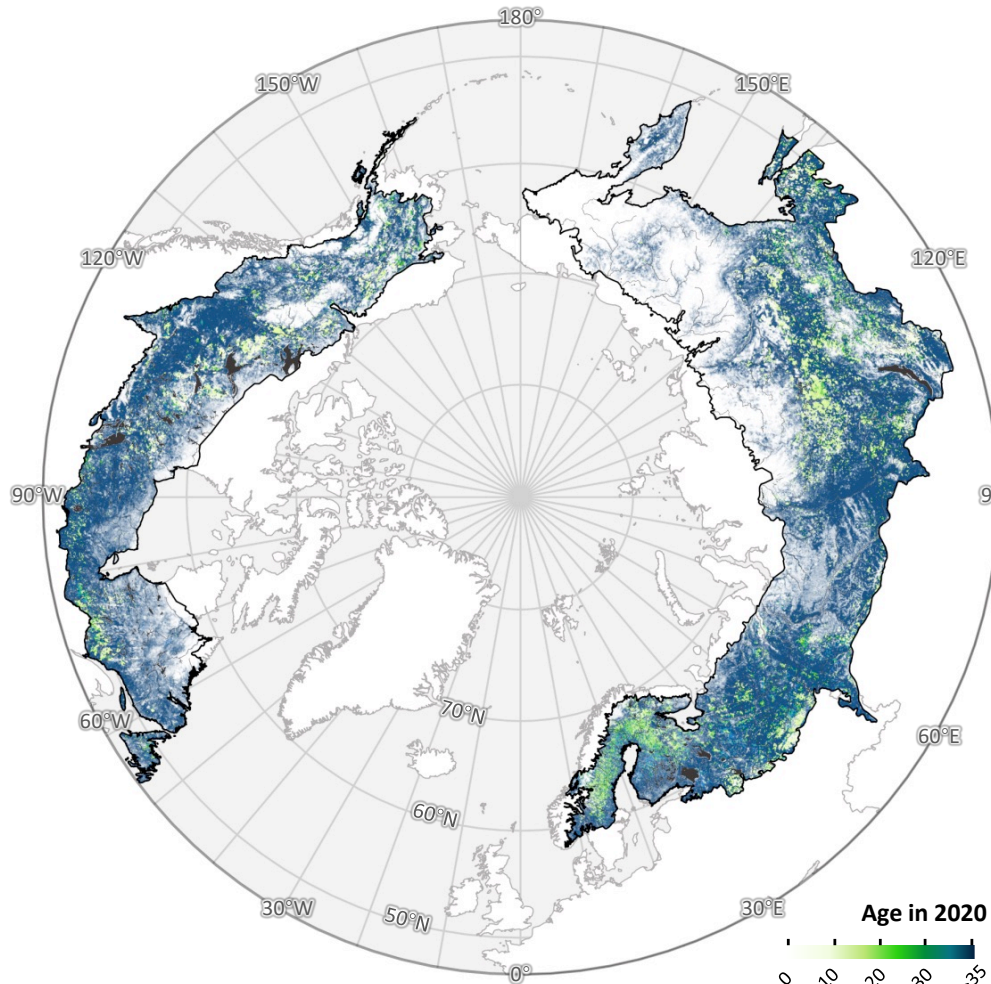
231 **3.3. The distribution of boreal forest age**

232 Most of the boreal forest—8.19 million km<sup>2</sup>, or 47.5% of the region—is older than can be directly measured from the  
233 satellite record (Fig. 4). Tree cover in these older stands was already established by the beginning of the Landsat  
234 observation period in 1985, and the slow rates of biomass accumulation in boreal ecosystems further complicate the  
235 detection of recent forest establishment (Fig. S15). However, the age of younger stands can be estimated by subtracting  
236 the year of first detected forest cover from 2020. The forest age estimator showed a root mean square error (RMSE)  
237 of 17.46 years and a mean bias of −3.27 years relative to reference data. These errors indicate that while the age maps  
238 capture broad spatial patterns and distributions, they should not be interpreted as precise pixel-level predictions.  
239 Instead, the results are most reliable when aggregated to regional or biome scales, where random errors are reduced.

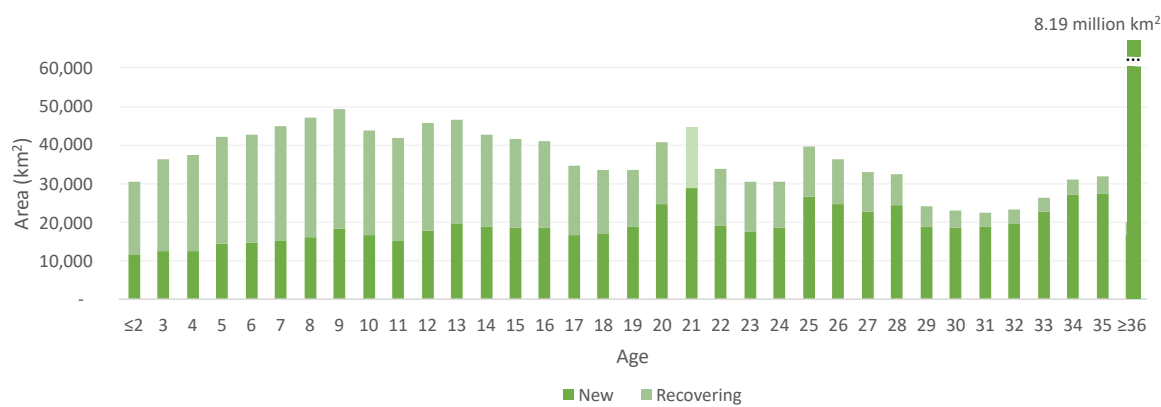
240 Of the forested area present in 1985, 0.5 million km<sup>2</sup>—representing 5.29% of standing forests—was disturbed  
241 during the study period and recovered to forest by 2020. Recovering forests, combined with “new” forests gained  
242 during the Landsat era, produced a weak modal age class centered between 9 and 21 years, with a notable lapse in the  
243 youngest age classes. These young forests were concentrated in regions of intensive silviculture, including industrial  
244 plantations in Scandinavia (Henttonen et al., 2017; Liski et al., 2003; Ågren et al., 2008), and in areas recovering from  
245 wildfire. The latter trend is corroborated by reports of increasing burn frequency and extent in Siberia since the late  
246 20th century (Kharuk et al., 2021), which has driven a rising proportion of recovering forest younger than 20 years.

247

248



249



250

251 **Fig. 4.** Spatial distribution of stand age (top) across the boreal ecoregion and frequency distribution of boreal stand age in  
 252 2020 (bottom). Forest age-class distribution is defined as years since establishment of pixels identified as forest in 2020.  
 253 “New” forests were identified as pixels with forest cover following a gain but no prior forest cover or loss earlier in the time  
 254 series within a 150-m radius (5 pixels) over the observable period (1984 – 2020); “recovering” forests were identified as  
 255 pixels with forest cover following a gain where a forest loss had been observed previously in the series (Supplemental  
 256 Information).

257

258 **4 Discussion**

259 The expansion and redistribution of boreal tree cover documented in this study has direct implications for the region's  
260 role in the global carbon cycle. Between 1985 and 2020, boreal tree cover increased by 0.844 million km<sup>2</sup> and shifted  
261 northward by over 0.4° in median latitude, with gains concentrated at the biome's northern margin and net expansion  
262 observed across most latitudes. These changes are not only spatially extensive but demographically consequential:  
263 they reflect a growing fraction of young forests with distinct structural and functional attributes that position them as  
264 dynamic agents of carbon sequestration. Understanding the contribution of these forests to current and future carbon  
265 stocks is essential for anticipating the net climate feedbacks emerging from boreal ecosystems.

266 Recent models relating forest age to biomass dynamics suggest that shifting age structure will substantially  
267 influence the boreal region's contribution to the global carbon budget in the coming decades. Young forests already  
268 contribute significantly to the region's carbon sink (Pan et al., 2011). Forest age estimates carry substantial uncertainty  
269 (RMSE ≈ 17 years), limiting their precision at the pixel scale. They remain useful for identifying large-scale patterns  
270 and average age structures, but future work will be required to reduce error and quantify regional biases. Forests with  
271 known stand ages (less than 36 years since disturbance) hold between 1.1 and 5.9 Pg C in aboveground biomass, based  
272 on global growth models (Cook-Patton et al., 2020). The ages of forests where no disturbance was observed during  
273 the satellite era remain unknown, but plausible aboveground carbon stocks in these older stands can be bracketed  
274 between a low-end scenario assuming 36 years of age (19.1–58.4 Pg C) and a high-end scenario assuming 300 years  
275 (42.4–89.2 Pg C). Based on these estimates, forests younger than 36 years of age comprise 1.35–14.20% of the total  
276 boreal aboveground biomass carbon stock—consistent with their 15.4% share of total forest area. Including  
277 belowground biomass would raise these values by approximately 25%, based on a mean global root:shoot ratio of  
278 0.25 (Huang et al., 2021).

279 If allowed to mature without further disturbance, these young forests could sequester an additional 2.3–  
280 3.8 Pg C in aboveground biomass. Forests newly established during the observation period contribute between 0.8  
281 and 3.5 Pg C today, exceeding the 0.3–2.4 Pg C held in forests recovering from recorded disturbances. Over the next  
282 36 years, new forests represent a potential additional aboveground sink of 1.3–2.0 Pg C (0.036–0.18 Pg C yr<sup>-1</sup>),  
283 compared to 1.0–1.8 Pg C (0.028–0.05 Pg C yr<sup>-1</sup>) from recovering forests. This distinction reflects both the greater  
284 area occupied by new forests (7.6% vs. 6.7%) and their older mean stand age. These findings support recent  
285 observations by Neigh et al. (2025), who reported a disproportionately large contribution of young, regrowing stands  
286 to carbon storage in the Russian boreal.

287 The additional carbon in new forests could help offset warming-induced increases in boreal ecosystem  
288 respiration, which have been estimated between 5 and 28 Pg C from 1985 to 2020 (Fig. S16). Both climate warming  
289 and carbon dioxide (CO<sub>2</sub>) fertilization are expected to enhance productivity (Norby and Zak, 2011), and the spatial  
290 pattern of observed tree-cover growth aligns with model predictions of increased seasonal CO<sub>2</sub> exchange above 40°N  
291 (Forkel et al., 2016). However, several mechanisms may limit this offset. First, temperature sensitivity of respiration  
292 can itself be temperature-dependent (Koven et al., 2017). Second, carbon accumulation rates decline with forest age  
293 (Odum, 1969). Third, thawing of permafrost can release substantial legacy carbon stocks (Schuur et al., 2015). Fourth,

294 increases in fire and harvest activity may reverse regional gains in biomass (Gauthier et al., 2015; Kharuk et al., 2021).  
295 Compositional and functional transitions may also alter sink dynamics (Montesano et al., 2024; Xi et al., 2024).

296 The long-term persistence of tree-cover expansion depends not only on productivity, but also on the capacity  
297 of boreal soils to support woody vegetation. It remains uncertain whether boreal soils—especially under changing  
298 permafrost regimes—can structurally sustain expanded forest cover (Koven, 2013). Additional uncertainty stems from  
299 the rising role of anthropogenic fire in some parts of the boreal zone (Doerr and Santin, 2016; Mollicone et al., 2006).  
300 Our biomass estimates are derived from models for natural forests and do not account for differences between managed  
301 and unmanaged systems (Kuuluvainen and Gauthier, 2018) or for anticipated changes in fire regimes.

302 While expansion of tree cover may imply increased carbon storage, nonlinear biodiversity responses to  
303 warming complicate projections. Enhanced taxonomic and functional diversity may improve ecological resilience (Xi  
304 et al., 2024), but these benefits are constrained by the growing frequency of climatic extremes. Moreover, biodiversity-  
305 related feedbacks on carbon balance remain difficult to predict under scenarios of increasing disturbance. Ultimately,  
306 all of these processes—forest growth, mortality, disturbance, and compositional change—are already underway across  
307 the boreal biome. Quantifying the balance of autotrophic and heterotrophic carbon fluxes remains critical to  
308 understanding and managing the global climate system.

309 While our calibration was stratified across ecological and topographic gradients to minimize overfitting, more  
310 stringent tests could be obtained by withholding subsets of the reference data (e.g., complete LVIS flightlines or high-  
311 resolution imagery tiles) within specific ecozones and revalidating predictions at those sites. Such “leave-tile-out”  
312 cross-validation would provide a direct assessment of model transferability at biome boundaries, including ecotones.  
313 A limitation is the absence of temporally repeated reference data, which prevents direct assessment of stability (bias  
314 drift). Our calibration and annual compositing reduce some risks, but nonstationary, unaccounted-for sensor  
315 differences, phenological shifts, and atmospheric noise remain possible contributors to temporal bias.

316 The accuracy of the reference datasets themselves warrants consideration. Montesano et al. (2023) showed  
317 that LVIS canopy heights agree closely with NASA G-LiHT airborne LiDAR, with coefficients of determination ( $R^2$ )  
318 up to 0.87 and root mean square errors of approximately 1–2 m depending on canopy cover and temporal offset. G-  
319 LiHT, with its high point density and small footprint, is widely regarded as a reference standard, though its own  
320 absolute error was not quantified in that study. For high-resolution optical reference data (QuickBird imagery, Google  
321 Earth interpretations), prior work (Montesano et al. 2009, 2016) demonstrated their utility in validating coarse-  
322 resolution products but also did not report independent accuracy or inter-observer precision. These limitations  
323 highlight the need for future work to establish formal error budgets for reference datasets, while affirming that they  
324 provide the best available benchmarks for tree cover calibration and validation.

## 325 **Summary and Conclusions**

326 This pan-boreal assessment provides the strongest empirical confirmation to date of a northward shift in boreal tree  
327 cover, long hypothesized by climate–vegetation models. By retrieving the longest, highest-resolution, and most  
328 spatially complete record of calibrated boreal tree cover available, we applied machine learning to the Landsat 4, 5, 7,  
329 and 8 surface reflectance archives to reconstruct annual, 30-m maps of forest change from 1985 to 2020. Time-series

330 analysis of  $1.9 \times 10^8$  pixels revealed widespread increases in tree-cover density and a poleward shift in forest  
331 distribution, occurring despite relatively stable disturbance rates across the biome.

332 Although the net trends are globally significant, they mask substantial geographic and temporal  
333 heterogeneity, as well as complexity in the ecological processes underlying forest change. These results underscore  
334 the need for high-resolution, disturbance-aware metrics to supplement NDVI-based assessments, particularly in  
335 climatically sensitive boreal transition zones (Yan et al., 2024). A more complete understanding of boreal forest  
336 dynamics will require integration of satellite time series with field-based measurements of canopy structure and the  
337 environmental drivers of growth, mortality, and species turnover. Moreover, translating the resulting information into  
338 action to forestall and adapt to climate change will require effective communication across scientific, government,  
339 and commercial domains of human activity.

#### 340 **Acknowledgments**

341 This research was supported by the NASA Carbon Cycle Science Program (NNH16ZDA001N-CARBON), National  
342 Science Foundation Arctic System Science Program (1604105), and NASA ABoVE (80NSSC19M0112). Satellite  
343 image processing was performed by terraPulse, Inc. on Amazon Web Services (AWS). Reference data for calibration  
344 and validation was produced on the NASA Goddard Spaceflight Center ADAPT and HEC clusters. Aaron Wells  
345 (ABR, Inc.), Celio De Sousa (NASA Goddard Space Flight Center, URSA, Inc.), and Jaime Nickeson (NASA  
346 Goddard Space Flight Center, SSAI, Inc.) contributed reference observations of forest cover and disturbance.  
347 Resources supporting this work were provided by the NASA High-End Computing Program through the NASA Center  
348 for Climate Simulation at Goddard Space Flight Center.

#### 349 **Data availability**

350 The data for this paper is made available online at <https://www.terrapulse.com/terraView/ccs>.

#### 351 **Author Contributions**

352 MF and JS designed and developed the tree-cover and forest-change algorithms. PM, PW, and MM conducted the  
353 validation and calibration. CN and PM co-edited the manuscript, CN secured research funding to conduct the  
354 study. BP commented on the final manuscript. NC and LC conducted the carbon impact analysis. NC conducted the  
355 ecosystem respiration analysis. SC developed the platform on AWS. MW, WW, and AE interpreted the validation  
356 dataset. JS conceived the study and compiled the manuscript with contributions from all coauthors.

#### 357 **Competing interests**

358 The author declares that there are no competing interests.

359 **References**

360 Ågren, G. I., Hyvönen, R., and Nilsson, T.: Are Swedish forest soils sinks or sources for CO<sub>2</sub>—model analyses based  
361 on forest inventory data, *Biogeochemistry*, 89, 139–149, <https://doi.org/10.1007/s10533-007-9121-0>, 2008.

362 Baltzer, J. L., Alexander, H. D., Greaves, H. E., Boulanger, Y., Gauthier, S., Fuller, M. M., and Beck, P. S. A.:  
363 Increasing fire and the decline of fire-adapted black spruce in the boreal forest, *Proc. Natl. Acad. Sci. USA*, 118,  
364 e2024872118, <https://doi.org/10.1073/pnas.2024872118>, 2021.

365 Beck, P. S. A., Juday, G. P., Alix, C., Barber, V. A., Winslow, S. E., Sousa, E. E., Heiser, P., Herriges, J. D., and  
366 Goetz, S. J.: Changes in forest productivity across Alaska consistent with biome shift, *Ecol. Lett.*, 14, 373–379,  
367 <https://doi.org/10.1111/j.1461-0248.2011.01598.x>, 2011.

368 Berner, L. T., and Goetz, S. J.: Satellite observations document trends consistent with a boreal forest biome shift,  
369 *Glob. Change Biol.*, 28, 3275–3292, <https://doi.org/10.1111/gcb.16100>, 2022.

370 Betts, R. A.: Offset of the potential carbon sink from boreal forestation by decreases in surface albedo, *Nature*, 408,  
371 187–190, <https://doi.org/10.1038/35041545>, 2000.

372 Bonan, G. B.: Forests and climate change: Forcings, feedbacks, and the climate benefits of forests, *Science*, 320,  
373 1444–1449, <https://doi.org/10.1126/science.1155121>, 2008.

374 Boulanger, Y., and Arseneault, D.: Spruce budworm outbreaks in eastern Quebec over the last 450 years, *Can. J. For.  
375 Res.*, 34, 1035–1043, <https://doi.org/10.1139/x03-269>, 2004.

376 Brice, M., Boucher, Y., Girardin, M. P., Marchand, W., Tremblay, J.-P., and Krause, C.: Moderate disturbances  
377 accelerate forest transition dynamics under climate change in the temperate–boreal ecotone of eastern North America,  
378 *Glob. Change Biol.*, 26, 4418–4435, <https://doi.org/10.1111/gcb.15115>, 2020.

379 Bunn, A. G., and Goetz, S. J.: Trends in satellite-observed circumpolar photosynthetic activity from 1982 to 2003:  
380 The influence of seasonality, cover type, and vegetation density, *Earth Interact.*, 10, 1–19,  
381 <https://doi.org/10.1175/EI190.1>, 2006.

382 Carroll, M., DiMiceli, C., Sohlberg, R., Huang, C., and Hansen, M. C.: MODIS Vegetative Cover Conversion and  
383 Vegetation Continuous Fields, in: *Land Remote Sensing and Global Environmental Change: NASA’s Earth Observing  
384 System and the Science of ASTER and MODIS*, edited by: Ramachandran, B., Justice, C. O., and Abrams, M. J., 725–  
385 745, Springer, New York, NY, [https://doi.org/10.1007/978-1-4419-6749-7\\_32](https://doi.org/10.1007/978-1-4419-6749-7_32), 2011.

386 Chen, D., Loboda, T. V., He, T., Zhang, Y., and Liang, S.: Strong cooling induced by stand-replacing fires through  
387 albedo in Siberian larch forests, *Sci. Rep.*, 8, 4821, <https://doi.org/10.1038/s41598-018-23050-9>, 2018.

388 Ciais, P., Yao, Y., Gasser, T., Baccini, A., Wang, Y., Lauerwald, R., Peng, S., Bastos, A., Cescatti, A., and Yue, C.:  
389 Five decades of northern land carbon uptake revealed by the interhemispheric CO<sub>2</sub> gradient, *Nature*, 568, 221–225,  
390 <https://doi.org/10.1038/s41586-019-1078-6>, 2019.

391 Cook-Patton, S. C., Leavitt, S. M., Gibbs, D., Harris, N. L., Lister, K., Anderson-Teixeira, K. J., Briggs, R. D.,  
392 Chazdon, R. L., Crowther, T. W., and Ellis, P. W.: Mapping carbon accumulation potential from global natural forest  
393 regrowth, *Nature*, 585, 545–550, <https://doi.org/10.1038/s41586-020-2686-x>, 2020.

394 Dial, R. J., Beamer, J. P., McDowell, P. D., Herriott, I. C., Milne, B. T., Giardina, C. P., and Sullivan, P. F.: Arctic  
395 sea ice retreat fuels boreal forest advance, *Science*, 383, 877–884, <https://doi.org/10.1126/science.adj0832>, 2024.

396 Dial, R. J., Maher, C. T., Hewitt, R. E., and Sullivan, P. F.: Sufficient conditions for rapid range expansion of a boreal  
397 conifer, *Nature*, 608, 546–551, <https://doi.org/10.1038/s41586-022-05066-4>, 2022.

398 Dinerstein, E., Olson, D., Joshi, A., Vynne, C., Burgess, N. D., Wikramanayake, E., Hahn, N., Palminteri, S., Hedao,  
399 P., and Noss, R.: An ecoregion-based approach to protecting half the terrestrial realm, *BioScience*, 67, 534–545,  
400 <https://doi.org/10.1093/biosci/bix014>, 2017.

401 Doerr, S. H., and Santín, C.: Global trends in wildfire and its impacts: perceptions versus realities in a changing world,  
402 *Philos. Trans. R. Soc. B Biol. Sci.*, 371, 20150345, <https://doi.org/10.1098/rstb.2015.0345>, 2016.

403 Elmendorf, S. C., Henry, G. H. R., Hollister, R. D., Björk, R. G., Bjorkman, A. D., Callaghan, T. V., and Collier, L.  
404 S.: Plot-scale evidence of tundra vegetation change and links to recent summer warming, *Nat. Clim. Change*, 2, 453–  
405 457, <https://doi.org/10.1038/nclimate1465>, 2012.

406 Fan, L., Wigneron, J.-P., Ciais, P., Chave, J., Brandt, M., Sitch, S., Yue, C., Bastos, A., Li, X., Qin, Y., Yuan, W.,  
407 Schepaschenko, D., Mukhortova, L., Li, X., Liu, X., Wang, M., Frappart, F., Xiao, X., Chen, J., ... Fensholt, R.:  
408 Siberian carbon sink reduced by forest disturbances. *Nature Geoscience*, 16(1), 56–62.  
409 <https://doi.org/10.1038/s41561-022-01087-x>, 2023

410 Forkel, M., Carvalhais, N., Rödenbeck, C., Keeling, R., Heimann, M., Thonicke, K., Reichstein, M., and High-  
411 Latitude Ecosystem Modeling Group: Enhanced seasonal CO<sub>2</sub> exchange caused by amplified plant productivity in  
412 northern ecosystems, *Science*, 351, 696–699, <https://doi.org/10.1126/science.aac4971>, 2016.

413 Frost, G. V., and Epstein, H. E.: Tall shrub and tree expansion in Siberian tundra ecotones since the 1960s, *Glob.*  
414 *Change Biol.*, 20, 1264–1277, <https://doi.org/10.1111/gcb.12406>, 2014.

415 Gauthier, S., Bernier, P., Kuuluvainen, T., Shvidenko, A. Z., and Schepaschenko, D. G.: Boreal forest health and  
416 global change, *Science*, 349, 819–822, <https://doi.org/10.1126/science.aaa9092>, 2015.

417 Guay, K. C., Beck, P. S. A., Berner, L. T., Goetz, S. J., Baccini, A., and Buermann, W.: Vegetation productivity  
418 patterns at high northern latitudes: a multi-sensor satellite data assessment, *Glob. Change Biol.*, 20, 3147–3158,  
419 <https://doi.org/10.1111/gcb.12647>, 2014.

420 Henttonen, H. M., Nöjd, P., and Mäkinen, H.: Environment-induced growth changes in the Finnish forests during  
421 1971–2010 – An analysis based on National Forest Inventory, *For. Ecol. Manag.*, 386, 22–36,  
422 <https://doi.org/10.1016/j.foreco.2016.12.021>, 2017.

423 Hofgaard, A., Dalen, L., and Hytteborn, H.: Tree recruitment above the treeline and potential for climate-driven  
424 treeline change, *J. Veg. Sci.*, 20, 1133–1144, <https://doi.org/10.1111/j.1654-1103.2009.01106.x>, 2009.

425 Holtmeier, F.-K., and Broll, G.: Sensitivity and response of northern hemisphere altitudinal and polar treelines to  
426 environmental change at landscape and local scales, *Glob. Ecol. Biogeogr.*, 14, 395–410,  
427 <https://doi.org/10.1111/j.1466-822X.2005.00168.x>, 2005.

428 Huang, Y., Crowther, T. W., and Maynard, D. S.: A global map of root biomass across the world's forests, *Earth Syst.*  
429 *Sci. Data*, 13, 4263–4274, <https://doi.org/10.5194/essd-13-4263-2021>, 2021.

430 IPCC: Climate Change Synthesis Report, IPCC, Geneva, Switzerland, 2014.

431 IPCC: Global Warming of 1.5°C, IPCC Special Report, 2018.

432 IPCC: Climate Change Synthesis Report. IPCC, Geneva, Switzerland, 2023.

433 Ju, J., and Masek, J. G.: The vegetation greenness trend in Canada and US Alaska from 1984–2012 Landsat data,  
434 *Remote Sens. Environ.*, 176, 1–16, <https://doi.org/10.1016/j.rse.2016.01.001>, 2016.

435 Kajii, Y., Kato, S., Streets, D. G., Tsai, N. Y., Shibata, T., Matsumoto, J., and Kajino, M.: Boreal forest fires in Siberia  
436 in 1998: Estimation of area burned and emissions of pollutants by advanced very high resolution radiometer satellite  
437 data, *J. Geophys. Res. Atmospheres*, 107, ACH 4-1–ACH 4-8, <https://doi.org/10.1029/2001JD001078>, 2002.

438 Kharuk, V. I., Ponomarev, E. I., Ivanova, G. A., Dvinskaya, M. L., Coogan, S. C. P., and Flannigan, M. D.: Wildfires  
439 in the Siberian taiga, *Ambio*, <https://doi.org/10.1007/s13280-020-01490-x>, 2021.

440 Koven, C. D.: Boreal carbon loss due to poleward shift in low-carbon ecosystems, *Nat. Geosci.*, 6, 452–456,  
441 <https://doi.org/10.1038/ngeo1801>, 2013.

442 Koven, C. D., Hugelius, G., Lawrence, D. M., and Wieder, W. R.: Higher climatological temperature sensitivity of  
443 soil carbon in cold than warm climates, *Nat. Clim. Change*, 7, 817–822, <https://doi.org/10.1038/nclimate3421>, 2017.

444 Krylov, A., McCarty, J. L., Potapov, P., Loboda, T., Tyukavina, A., Turubanova, S., and Hansen, M. C.: Remote  
445 sensing estimates of stand-replacement fires in Russia, 2002–2011, *Environ. Res. Lett.*, 9, 105007,  
446 <https://doi.org/10.1088/1748-9326/9/10/105007>, 2014.

447 Kuuluvainen, T., and Gauthier, S.: Young and old forest in the boreal: critical stages of ecosystem dynamics and  
448 management under global change, *For. Ecosyst.*, 5, 26, <https://doi.org/10.1186/s40663-018-0149-8>, 2018.

449 Liski, J., Perruchoud, D., Karjalainen, T., and Poulton, P.: Increased carbon sink in temperate and boreal forests, *Clim.*  
450 *Change*, 61, 89–109, <https://doi.org/10.1023/A:1026368803516>, 2003.

451 Mack, M. C., Walker, X. J., Johnstone, J. F., Alexander, H. D., Melvin, A. M., Miller, S. N., and Goetz, S. J.: Carbon  
452 loss from boreal forest wildfires offset by increased dominance of deciduous trees, *Science*, 372, 280–283,  
453 <https://doi.org/10.1126/science.abf3903>, 2021.

454 Massey, R., Walker, X. J., Mack, M. C., Johnstone, J. F., Miller, S. N., and Goetz, S. J.: Forest composition change  
455 and biophysical climate feedbacks across boreal North America, *Nat. Clim. Change*, 13, 1368–1375,  
456 <https://doi.org/10.1038/s41558-023-01826-4>, 2023.

457 McManus, K. M., Morton, D. C., Masek, J. G., Wang, D., Sexton, J. O., and Nagol, J.: Satellite-based evidence for  
458 shrub and graminoid tundra expansion in northern Quebec from 1986 to 2010, *Glob. Change Biol.*, 18, 2313–2323,  
459 <https://doi.org/10.1111/j.1365-2486.2012.02708.x>, 2012.

460 Meddens, A. J. H., Hicke, J. A., and Ferguson, C. A.: Spatiotemporal patterns of observed bark beetle-caused tree  
461 mortality in British Columbia and the western United States, *Ecol. Appl.*, 22, 1876–1891, <https://doi.org/10.1890/11-1785.1>, 2012.

463 Mekonnen, Z. A., Riley, W. J., Randerson, J. T., Grant, R. F., and Rogers, B. M.: Expansion of high-latitude deciduous  
464 forests driven by interactions between climate warming and fire, *Nat. Plants*, 5, 952–958,  
465 <https://doi.org/10.1038/s41477-019-0495-6>, 2019.

466 Mollicone, D., Eva, H. D., and Achard, F.: Human role in Russian wildfires, *Nature*, 440, 436–437,  
467 <https://doi.org/10.1038/440436a>, 2006.

468 Montesano, P. M., Frost, M., Li, J., Carroll, M., Neigh, C. S. R., Macander, M. J., Sexton, J. O., & Frost, G. V.: A  
469 shift in transitional forests of the North American boreal will persist through 2100, *Nature Communications: Earth*  
470 and *Environment*, 5, 1, <https://doi.org/10.1038/s43247-024-01454-z>, 2024.

471 Montesano, P. M., Neigh, C. S. R., Macander, M. J., Wagner, W., Duncanson, L. I., Wang, P., Sexton, J. O., Miller,  
472 C. E., & Armstrong, A. H.: Patterns of regional site index across a North American boreal forest gradient.  
473 *Environmental Research Letters*, 18(7), 075006. <https://doi.org/10.1088/1748-9326/acdcab>, 2023

474 Montesano, P. M., Nelson, R., Sun, G., Margolis, H., Kerber, A., & Ranson, K. J.: MODIS tree cover validation for  
475 the circumpolar taiga–tundra transition zone. *Remote Sensing of Environment*, 113(10), 2130–2141.  
476 <https://doi.org/10.1016/j.rse.2009.05.021>, 2009

477 Montesano, P. M., Sun, G., Dubayah, R. O., & Ranson, K. J.: Spaceborne potential for examining taiga–tundra ecotone  
478 form and vulnerability. *Biogeosciences*, 13(13), 3847–3861. <https://doi.org/10.5194/bg-13-3847-2016>, 2016

479 Neigh, C. S. R., Tucker, C. J., and Townshend, J. R. G.: North American vegetation dynamics observed with multi-  
480 resolution satellite data, *Remote Sens. Environ.*, 112, 1749–1772, <https://doi.org/10.1016/j.rse.2007.08.018>, 2008.

481 Neigh, C. S. R., Nelson, R. F., Ranson, K. J., Margolis, H. A., Montesano, P. M., Sun, G., and Goetz, S. J.: Taking  
482 stock of circumboreal forest carbon with ground measurements, airborne and spaceborne LiDAR, *Remote Sens.*  
483 *Environ.*, 137, 274–287, <https://doi.org/10.1016/j.rse.2013.06.019>, 2013.

484 Neigh, C., Montesano, P. M., Sexton, J. O., Wooten, M., Wagner, W., Feng, M., Carvalhais, N., Calle, L., & Carroll,  
485 M. L.: Russian forests show strong potential for young forest growth, *Nature Communications: Earth and*  
486 *Environment*, 6, 1, <https://doi.org/10.1038/s43247-025-02006-9>, 2025.

487 Norby, R. J., and Zak, D. R.: Ecological lessons from Free-Air CO<sub>2</sub> Enrichment (FACE) experiments, *Annu. Rev. Ecol. Evol. Syst.*, 42, 181–203, <https://doi.org/10.1146/annurev-ecolsys-102209-144647>, 2011.

488

489 Odum, E. P.: The strategy of ecosystem development, *Science*, 164, 262–270, <https://doi.org/10.1126/science.164.3877.262>, 1969.

490

491 Pan, Y., Birdsey, R. A., Fang, J., Houghton, R., Kauppi, P. E., Kurz, W. A., and Phillips, O. L.: A large and persistent carbon sink in the world's forests, *Science*, 333, 988–993, <https://doi.org/10.1126/science.1201609>, 2011.

492

493 Pan, Y., Birdsey, R. A., Phillips, O. L., Houghton, R. A., Fang, J., Kauppi, P. E., Keith, H., Kurz, W. A., Ito, A., Lewis, S. L., Nabuurs, G.-J., Shvidenko, A., Hashimoto, S., Lerink, B., Schepaschenko, D., Castanho, A., & Murdiyarso, D.: The enduring world forest carbon sink. *Nature*, 631(8021), 563–569. <https://doi.org/10.1038/s41586-024-07602-x>, 2024

494

495

496

497 Piao, S., Wang, X., Ciais, P., Zhu, B., Wang, T., and Liu, J.: Characteristics, drivers and feedbacks of global greening, *Nat. Rev. Earth Environ.*, 1, 14–27, <https://doi.org/10.1038/s43017-019-0001-x>, 2020.

498

499 Randerson, J. T., Liu, H., Flanner, M. G., Chambers, S. D., Jin, Y., Hess, P. G., and Rasch, P. J.: The impact of boreal forest fire on climate warming, *Science*, 314, 1130–1132, <https://doi.org/10.1126/science.1132075>, 2006.

500

501 Rees, W. G., Stammer, F. M., Danks, F. S., and Vitebsky, P.: Is subarctic forest advance able to keep pace with climate change?, *Glob. Change Biol.*, 26, 3965–3977, <https://doi.org/10.1111/gcb.15181>, 2020.

502

503 Rotbarth, R., Walker, X. J., Mack, M. C., Goetz, S. J., Johnstone, J. F., and Miller, S. N.: Northern expansion is not compensating for southern declines in North American boreal forests, *Nature Communications*, 14, 3373, <https://doi.org/10.1038/s41467-023-39128-8>, 2023.

504

505

506 Sato, H., Kobayashi, H., Iwahana, G., and Ohta, T.: Endurance of larch forest ecosystems in eastern Siberia under warming trends, *Ecol. Evol.*, 6, 5690–5704, <https://doi.org/10.1002/ece3.2264>, 2016.

507

508 Scheffer, M., Hirota, M., Holmgren, M., van Nes, E. H., and Chapin, F. S.: Thresholds for boreal biome transitions, *Proc. Natl. Acad. Sci. USA*, 109, 21384–21389, <https://doi.org/10.1073/pnas.1219844110>, 2012.

509

510 Schuur, E. A. G., Abbott, B. W., Bowden, W. B., Brovkin, V., Camill, P., Davidson, E. A., and Hayes, D. J.: Climate change and the permafrost carbon feedback, *Nature*, 520, 171–179, <https://doi.org/10.1038/nature14338>, 2015.

511

512 Sexton, J. O., Noojipady, P., Song, X.-P., Feng, M., Song, D. X., Kim, D. H., and Hansen, M. C.: Global, 30-m resolution continuous fields of tree cover: Landsat-based rescaling of MODIS vegetation continuous fields with LiDAR-based estimates of error, *Int. J. Digit. Earth*, 6, 427–448, <https://doi.org/10.1080/17538947.2013.786146>, 2013.

513

514

515

516 Walker, X. J., Rogers, B. M., Baltzer, J. L., Baltzer, B., Barrett, M., Bourgeau-Chavez, L., and Mack, M. C.: Increasing wildfires threaten historic carbon sink of boreal forest soils, *Nature*, 572, 520–523, <https://doi.org/10.1038/s41586-019-1474-y>, 2019.

517

518

519 UNFCCC: Report of the Conference of the Parties on its Seventh Session, held at Marrakesh from 29 October to 10  
520 November 2001, Addendum Part Two, United Nations Framework Convention on Climate Change, 2002

521 Xi, Y., Zhang, W., Wei, F., Fang, Z., & Fensholt, R.: Boreal tree species diversity increases with global warming but  
522 is reversed by extremes, *Nature Plants*, <https://doi.org/10.1038/s41477-024-01794-w>, 2024.

523 Yan, Y., Piao, S., Hammond, W. M., Chen, A., Hong, S., Xu, H., Munson, S. M., Myneni, R. B., & Allen, C. D.:  
524 Climate-induced tree-mortality pulses are obscured by broad-scale and long-term greening, *Nature Ecology and*  
525 *Evolution*, <https://doi.org/10.1038/s41559-024-02372-1>, 2024.

526 Zhu, Z., Piao, S., Myneni, R. B., Huang, M., Zeng, Z., Canadell, J. G., and Ciais, P.: Greening of the Earth and its  
527 drivers, *Nat. Clim. Change*, 6, 791–795, <https://doi.org/10.1038/nclimate3004>, 2016.